

The Journal of Undergraduate Research in Physics

INTERFACING STUDENT TEMPERATURE LABS TO A COMPUTER NETWORK SYSTEM.....3

Rob Wamsley
University of Northern Colorado

THE EVALUATION OF A MECHANISM FOR IRRADIATION ENHANCED ADHESION.....9

John G. Bognar
Wright State University

THE WEISBUCH/ATLAN MODEL OF IMMUNE RESPONSE.....15

Ulrich Wiesner
Bergish Gladbach, West Germany

MONTE CARLO SIMULATION OF A HIGH PRESSURE PROPORTIONAL COUNTER.....19

Zoltan Egyed
Eotvos University, Budapest Hungary and Union College

SUPERIONIC-COVALENT PHASE TRANSITIONS IN ALLOYS OF Ag_3SI with Ag_3SBr23

Eric Moen, Greg Schurter and Ivan Wick
University of Wisconsin-Stevens Point

Post-Use Book Review - *Classical Mechanics* A. Douglas Davis *Dynamics of Particles and Systems, 2nd Ed.* Jerry B. Marion.....25

G. Douglas Meegan, Jr.
Guilford College

VOLUME 7, NUMBER 1

October 1988

Published by the Physics Department of Guilford College
for
The American Institute of Physics and The Society of Physics Students



THE JOURNAL OF UNDERGRADUATE RESEARCH IN PHYSICS

This journal is devoted to research work done by undergraduate students in physics and its related fields. It is to be a vehicle for the exchange of ideas and information by undergraduate students. Information for students wishing to submit manuscripts for possible inclusion in the Journal follows.

ELIGIBILITY

The author must have performed all work reported in the paper as an undergraduate. The subject matter of the paper is open to any area of pure or applied physics or physics related field.

SPONSORSHIP

Each paper must be sponsored by a full-time faculty member of the department in which the research was done. A letter from the sponsor, certifying that the work was done by the author as an undergraduate and the the sponsor is willing to be acknowledged in the paper, must accompany the manuscript if it is to be considered for publication.

SUBMISSION

Two copies of the manuscript, the letter from the sponsor and a telephone number where the author can be reached should be sent to:

Dr. Rexford E. Adelberger, Editor
THE JOURNAL OF UNDERGRADUATE
RESEARCH IN PHYSICS
Physics Department
Guilford College
Greensboro, NC 27410

FORM

The manuscript should be typed, double

spaced, on 8 1/2 x 11 inch sheets. Margins of about 1.5 inches should be left on the top, sides, and bottom of each page. Papers should be limited to fifteen pages of text in addition to an abstract (not to exceed 250 words) and appropriate drawings, pictures, and tables. Manuscripts may be submitted on a disk that can be read by a MacIntosh™. The files must be compatible with MacWrite™ or MicroSoft Word™. Illustrations should be in a MacDraw™ or MacPaint™ PICT format.

ILLUSTRATIONS

Line drawings should be made with black ink on plain white paper. Each figure or table must be on a separate sheet. Photographs must have a high gloss finish.

CAPTIONS

A brief caption should be provided for each illustration or table, but it should not be part of the figure. The captions should be listed together at the end of the manuscript

EQUATIONS

Equations should appear on separate lines, and may be written in black ink.

FOOTNOTES

Footnotes should be typed, double spaced and grouped together in sequence at the end of the manuscript.

SUBSCRIPTION INFORMATION

The Journal is published bianually, with issue one appearing in October and issue two in April of the next year. There are two issues per volume.

TYPE OF SUBSCRIBER	PRICE PER VOLUME
Individual.....	\$US 5.00
Institution.....	\$US 10.00

Foreign subscribers add \$US 2.00 for surface postage, \$US 10.00 for air freight.

To receive a subscription, send your name, address, and check made out to **The Journal of Undergraduate Research in Physics**

(JURP) to the editorial office:

JURP
Physics Department
Guilford College
Greensboro, NC 27410

Back issues may be purchased by sending \$US 15.00 per volume to the editorial office.

The *Journal of Undergraduate Research in Physics* is published by the Physics Department of Guilford College for the American Institute of Physics and the Society of Physics. **ISSN 0731-3764**

VOLUME 7

1988-89

**The Journal of
Undergraduate Research
in Physics**



*Published by the Physics Department
of Guilford College
for*

*The American Institute of Physics
and
The Society of Physics Students*

ISSN 0731 - 3764

INTERFACING STUDENT TEMPERATURE LABS TO A COMPUTER NETWORK SYSTEM

Rob Wamsley ^a
Department of Physics
University of Northern Colorado
Greeley, CO 80639

ABSTRACT

This research involved interfacing student temperature labs to a computer network system which consisted of a central computer and a number of node computers, one at each student lab table. As part of the design, software was developed to provide communication between the computers in the network system and to process data. Auxiliary circuitry was developed to establish a serial interface between the central computer and a digital thermometer unit. The computer causes the thermometer unit to poll through the temperature probes at each student station. Data are sent through the network to the appropriate node computer for display and recording. This system provides excellent operation at low

INTRODUCTION

The objective of this phase of an ongoing project at the University of Northern Colorado was to interface undergraduate student temperature laboratories to a computer network system. The specific experiments targeted by this project were: calorimetry, linear expansion due to heat and heat equivalent of work.

Calorimetry

In the calorimetry experiments, the students mix two substances of different temperatures, e.g. hot and cold water or hot aluminum shot and cold water. By measuring the masses of the substances and the temperatures before and after mixing, the student can calculate the specific heat of the substances. In other calorimetry experiments, the students can find the heat of fusion and the heat of vaporization of substances.

By making a computer control the experiments, the data can be taken more accurately and calculations can be speeded up. Another advantage of the computer controlled experiment is that the instructor can easily check the students' results by using the the computer to analyze the data at a later time.

Linear Expansion

For the linear expansion experiment, the student places a test rod (e.g. aluminum, brass, copper, etc.) in a bath of water or steam. The student measures the change in length of the rod as the temperature changes. The coefficient of expansion is calculated from this data. Usually it is only convenient to take readings of the total change in length of the rod between the initial and final temperature.

This experiment will benefit from computer interfacing in several ways. Since a more accurate thermometer with quicker response can be utilized, a reasonably full history of the temperature can be recorded. Methods of continuously reading the change in length of the rod using a linear variable differential transformer (LVDT) are currently under development ¹. The LVDT can be integrated with a temperature reading system such as described here to yield accurate data on the change of length versus temperature. The rapid plotting of data and least square fits using the computer are valuable consequences of this interfacing.

Joule's Experiment

To determine the heat equivalent of mechanical

work, the student hangs a weight from a string wrapped around a cylindrical container of water. The student turns the water container in a way such that the friction between the surface of the water container and the string is just enough to keep the weight from falling to the floor. The temperature of the water in the container will increase due to the work done against friction. The student measures the increase in the temperature. The energy needed to heat up the water is found by multiplying the change in temperature by the specific heat of water. The work done by the hanging weight is found by multiplying the weight by the distance traveled (circumference of the container times the number of turns) by turning the crank. The student verifies that the work done by turning the crank is equal to the energy which heats the water.

The number of revolutions the container has been turned is input into the computer with the temperature, providing x-y data for plotting and analyzing. This experiment benefits from the computer's facility in calculations and graphing the temperature versus time. This allows the student to see the temperature rise as work is done.

THE SYSTEM

Components

The accuracy of the computerized temperature measuring system is limited by the accuracy of the temperature measuring devices used. The thermometers currently used in student labs are calibrated to the nearest 1 C. Estimates can be made to about .5 C. Because of thermal delays and non-linearity, it is unlikely that readings from such thermometers are more accurate than ± 0.7 C. It is important to obtain accurate temperatures, as often the experiments require a knowledge of the difference between two temperatures. The accuracy problem can be helped by using a thermistor probe such as the Omega 661. It has a resolution of 0.1 C and can measure to a 0.4 C accuracy².

The computer interface system uses a network of seven Sinclair QL computers³, arranged as shown in Figure 1. Six of these computers, called "node computers", are at the existing lab benches. A seventh computer, with 512K expanded memory and tied to a disk drive, a printer and the temperature display unit, is designated to run the system. Network wiring uses coaxial cables. The temperature display unit is an Omega 661 thermistor-based

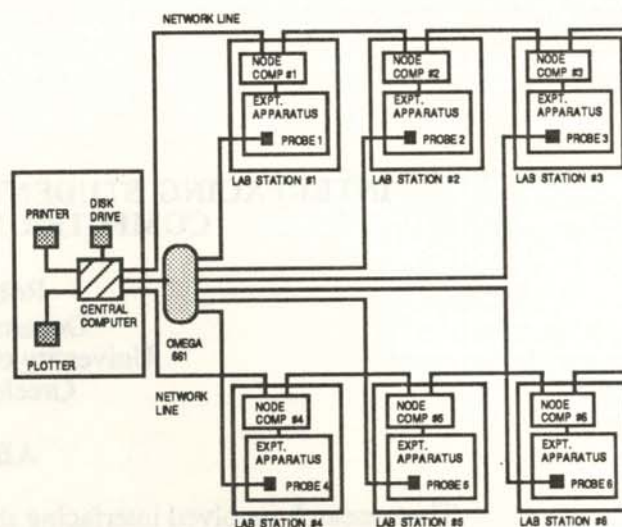


Figure 1

Networked computer system with individual temperature probes and a central Omega 661 Thermometer Unit.

thermometer unit 4. This system could be expanded to include more node computers.

The cost (1988) of an Omega 661, a computer, and a disk drive at each of six lab stations would be in excess of \$9,000. By using a network system, only one central Omega 661 and one disk drive interface at the central computer are needed. Each of the lab stations (nodes) will have a temperature sensing thermistor probe and a simplified QL computer, as shown in Figure 1. This method reduces the total cost of interfacing the temperature labs by nearly \$4,500. A word processor, a spread sheet and a data base are included in the system and can be loaded into the node computers from the central computer.

Programming

Networking programs already developed perform the tasks of starting up the network, transferring programs, acquiring data and saving numerical and graphical data. Copies of these programs are available on request⁵. The first program which is loaded and executed when the central computer is turned on is named "Boot". It is designed to load the networking programs, but also allows the user to view the directory of programs on the disk of the central computer or run other programs. The Boot program directs the start-up activities of the node computers in the network system. It then loads an

operating program into the node computers and a second operating program into the central computer.

The operating program loaded into the node computers, named "Node", allows each user at a lab station to view the central computer's entire directory of programs. The students can choose the correct program for the experiment they are conducting. When the students are finished with one experiment, the Node program will be reloaded and another choice made.

The operating program that is loaded into the central computer, named "central", controls all the communications between the central computer, the node computers, the disk drive and the printer. With this program, the central computer "listens" to the node computers. Upon request, the central computer can send the disk directory or program to a node computer. If a node computer operator requests a program that is not on the diskette, the central computer will send the "fnf" (file not found) program to the computer. The "fnf" program lets the user know that the file is not on the diskette and then reloads the "Node" program so that the user can view the directory and choose another program.

The node computer operator can elect to print the node screen display on the printer at the central computer (a process called a screen dump). To do this, the central computer sends a program called "NODEdump" to the node computers and merges "NETdump" with its current program. These two programs together accomplish the screen dump. After the screen dump, the central computer erases "NETdump" and waits for the next request from the node computers.

Data can be graphed from the lab station by running a program called "Graph". Data can be entered and edited. The user can choose a scale for the axes or have it done automatically. The program includes a least squares fit routine. After the display is complete, the user can print it out using a screen dump.

The program that acquires the data for temperature labs is called "Temp". It requests temperature readings from the Omega 661 display unit and stores the data. This program, not yet finished, will use a polling process to choose a lab station (or node) and to acquire and send the data from that

individual station.

Data Transfer

There are two ways that a lab station can get data from the Omega 661 display unit (see Figure 1). In both methods, the timing between temperature measurements is determined by the node computer.

The first method is to have the node computer request a temperature reading from the central computer by sending a request for data through the network. At the same time, the node sends its identification number so that the central computer knows which probe to select and where to send the data. The node computer then waits for the data to be sent to it. Once the central computer receives the request, it sends the information out over a serial port to the Omega 661 display unit. The auxiliary circuitry designed to interface the Omega 661 then selects the temperature probe of the appropriate lab station. The central computer then requests data from the Omega 661 which sends the data out in parallel ACSII form. This data is converted to serial form and sent to the central computer through its serial port. The central computer finally sends the data to the node computer over the network.

The second method for the lab station to receive its data is to have the central computer use a polling process. The process uses the same circuitry, but the central computer selects one lab station after another at a rapid rate and checks to see if that station has requested data. If so, it processes the request and moves on to the next lab station.

Equipment and Circuitry

The system (shown in Figure 2) uses Sinclair QL computers because they are equipped with network ports, have good graphic capabilities, are easy to program in SuperBASIC and make full use of the 7.5 MHz clock speed. The Omega 661 thermometer and display unit is used because it has excellent accuracy and produces an ASCII output in addition to the LED display of the temperature. The temperature is determined by measuring the current through a probe resistor. The Omega 661 is also used to power the circuitry of the interface. The main component of the interfacing circuitry is an Universal Asynchronous Receiver Transmitter (UART) used to convert between parallel and serial information.

The temperature measuring sequence begins when the computer sends a serial signal through the RS-

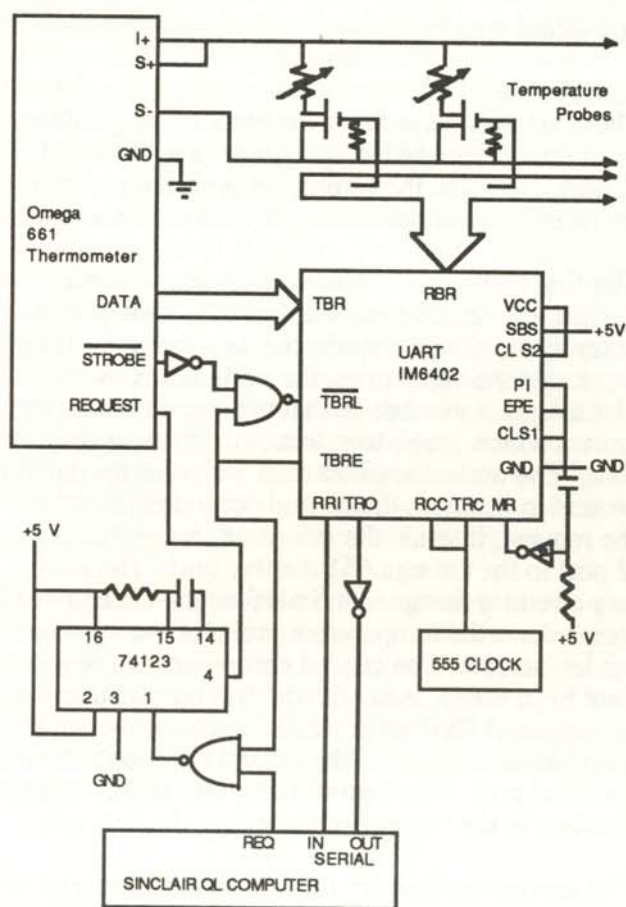


Figure 2

Interface circuitry for the individual probes, the Omega 661 thermometer unit and the central computer

232 port to the UART where it is converted to parallel data. The parallel signal has one high bit that corresponds to the specific lab station that is requesting service. This bit triggers a Metal Oxide Semiconductor Field Effect Transistor (MOSFET) which acts as an extremely low resistance electronic switch. The activated MOSFET allows current to flow through the selected temperature probe. At the same time that the computer sends the signal to select the temperature probe, it sends another signal to the interface circuitry to initiate the temperature conversion. When the Omega 661 reads the probe, it sends the temperature data out in parallel form to the UART. The UART converts this to serial data and sends it to the RS-232 port of the central computer, which sends the data back to the lab station computer via the network system.

Testing

The network programs were tested on a two computer (one as the central computer and the other as a node computer) one probe system. The programs functioned on the two computer system without error. The final system will have seven computers.

The limiting time factor of the system is the Omega 661. It takes 0.4 sec. to convert the resistance value of each thermistor to a binary signal. The cycle time for polling 6 stations then would be 2.4 seconds. This limits the degree to which the user can plan for readings to be taken at precise time intervals.

ACKNOWLEDGEMENTS

The author acknowledges valuable help from A. Loomis on the electronics for this project.

REFERENCES

- a) Current address: Department of Physics, University of Wisconsin, Madison, WI 53715.
- 1) A paper on the use of the LVDT to measure length in linear expansion as well as some other aspects of temperature labs is in preparation.
- 2) The 0.4 C accuracy of the Omega 661 unit is applicable for thermistor sensor probes. With Resistance Temperature Detectors, the accuracy is 0.3 C. However, these probes are more expensive and use a three wire connection which complicates the interface.
- 3) Sinclair QL (Quantum Leap) computers were developed in England. US dealers are Curry Computer, PO Box 5607, Glendale AZ 85312-5607; and Sharps Inc., Rt. 10, PO Box 459, Mechanicsville VA 23111. Periodicals on this computer include: *QL World*, 79 Petty France, London, England SW1H9ED; *The QL Report*, Curry Computer; and *Quantum Levels*, PO Box 64, Jefferson NH 03483. Information on SuperBASIC is contained in the computer instruction manual and in Jones, Jan, *QL SuperBASIC: The Definitive Handbook*, McGraw-Hill, London, 1985.
- 4) The Omega 661 is manufactured by Omega Engineering, Inc., One Omega Drive, Box 4047, Stamford CT 06907-0047. Extensive handbooks on temperature measurement are availa-

ble free from Omega.

- 5) A listing of the programs described in this article is available by writing to: W.L. Fadner, Department of Physics, University of Northern Colorado, Greeley, CO 80631.

FACULTY SPONSOR

Professor W.L. Fadner
Department of Physics
University of Northern Colorado
Greeley, CO 80631

THE EVALUATION OF A MECHANISM FOR IRRADIATION ENHANCED ADHESION

John G. Bognar
Physics Department
Wright State University
Dayton, OH 45435

ABSTRACT

Changes in thin film adhesion due to electron and proton irradiation were studied. Thin films of copper on quartz substrates were irradiated with electrons and protons of sufficient energy to cause damage in the form of point defects in the substrate material. The degree to which the interaction between charged point defects in the quartz and their image charges in the Cu film is the responsible mechanism for increased adhesion was investigated by determining which order of irradiation and film deposition resulted in the greatest change in adhesion. Irradiation of Cu films following deposition was found to be most effective. Diminished adhesion is associated with heating of the samples.

INTRODUCTION

Thin films have a vast number of uses including many electronic and optical applications¹. Solid state electronic devices are fabricated by deposition and modification of many thin layers of materials onto a substrate. Thin magnetic films are used to make the discs which serve as large volume memory storage devices in computers. Thin films are used to coat optical devices to alter their reflective behavior. Thus, improved adhesive strength between thin films and their substrates is of interest in many fields of science and technology.

It has been shown that increased adhesion can occur as result of ion irradiation^{2,3}. The increase in adhesion may result from three mechanisms caused by ion bombardment. One such mechanism may be the formation of a graded composition due to ion-beam mixing of the two materials at the interface. In this case, the heavy energetic ions deposit energy along their path leaving regions of very energetic atoms in their wake. The motion of these energetic atoms near the interface causes the atoms that make up each material to be mixed at the interface and to form a region of graded composition several tens of angstroms thick. (See Figure 1a.) The result is the absence of the abrupt interface that existed before the irradiation. When a force is ap-

plied to remove the film, the fracture which would normally propagate parallel to the abrupt interface and result in delamination, is distributed within the graded region. Thus, there is less chance of the fracture growing into a break along the interface. Electrons and protons were used in this study to avoid ion-beam mixing. The relatively small mass of these particles will favor the formation of point defects rather than the damage cascades involved in ion-beam mixing.

A second proposed mechanism for enhancing adhesion which can be caused by either ion or electron irradiation involves interfacial chemical bonding. (See Figure 1b.) In this case, the radiation causes ionization of atoms at the interface between each material in excess of any ionization due to the chemical state of the atoms. These ionized, or super-ionized atoms are therefore chemically active and can form numerous chemical bonds between the atoms of the film and the atoms of the substrate which would not form in thermo-chemical equilibrium⁴.

A third possible mechanism for improved adhesion caused by particle irradiation results from the formation of charged defects and their image charges⁵. The incident particles may cause a displace-

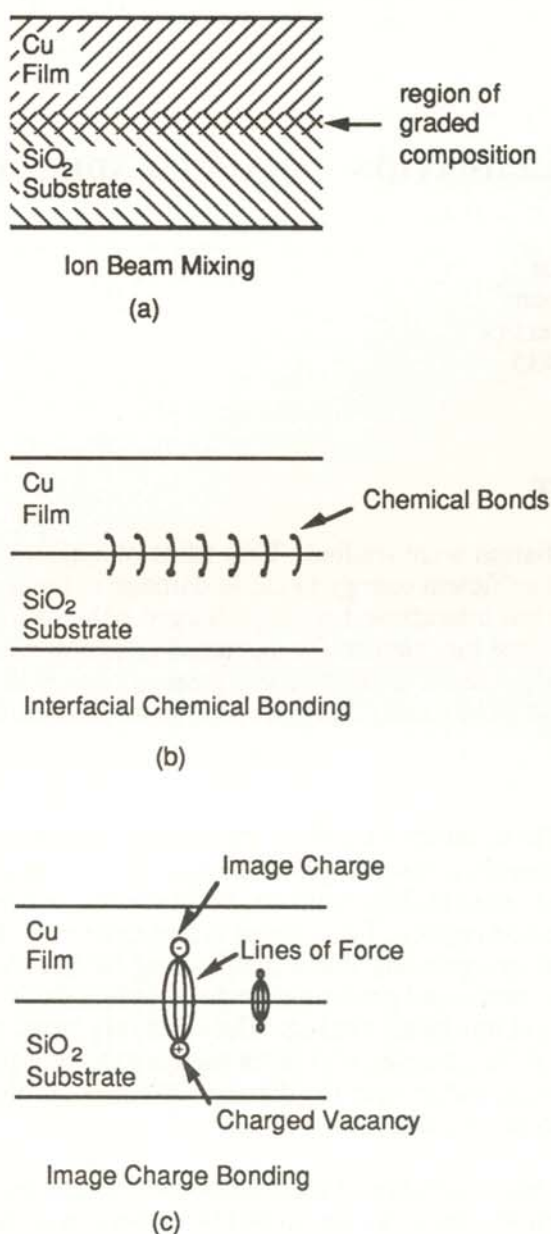


Figure 1

Three different mechanisms by which irradiation can improve adhesion; (a.) graded composition resulting from ion-beam mixing, (b.) chemical bonds formed from ionized constituents across the geometric interface, (c.) electrostatic attraction between charged defect and its image charge.

ment in the atoms in the substrate, leaving vacancies and interstitials. If the substrate atoms are ionically bonded, these defects are charged. When a metal film is present at the substrate surface, the charged defects induce a redistribution of free

charge in the metal film to keep the boundary between the metal film and substrate an equipotential surface. This is equivalent to placing a set of charges of equal magnitude and opposite sign equidistant from the set of charged defects on the opposite side of the interface, so that the interface region would again be an equipotential⁶. (See Figure 1c.)

Therefore, the existence of charged defects near the interface of a substrate will produce image charges in any conducting film deposited on the substrate. The attraction between the charged defects and their oppositely charged images will cause an increased adhesion between the film and the substrate.

We have investigated the degree to which image-charge bonding is responsible for an increased adhesion. Samples consisting of Cu on SiO₂ were chosen because this combination further reduces the possibility of not ion-beam mixing² and it has been shown that adhesion of this combination has been improved by electron irradiation⁷. Defects were introduced before and after film deposition. Since image charge bonding depends only on damage occurring in the substrate side of the interface, irradiation either before or after thin film deposition should bring about this mechanism.

PROCEDURE

One inch square slides of a-quartz with X-cut surface normal were cleaned with a solution of 5% hydrofluoric acid, 35% HNO₃, and 60% distilled water. This solution cleans the samples by smoothly etching surface layers of the material. A film of Cu was deposited by evaporation of chemically pure Cu wire onto quartz slides under a vacuum of 5×10^{-6} torr. The film thickness was approximately 1000 angstroms. Thickness was measured by use of a Dektak[®] profilometer.

One MeV electrons were provided by an electron Van de Graaf accelerator and 0.2 MeV protons were provided by a positive ion Van de Graaf accelerator. In a Van De Graaf accelerator, a rubber conveyor belt separates charge between a grounded base plate and an isolated "dome." The separated charge provides the electrostatic potential needed to accelerate charged particles. The belt also drives an alternator in the "dome" which provides electrical power to devices in the dome. In the electron Van de Graaf, the power is used to boil electrons off a

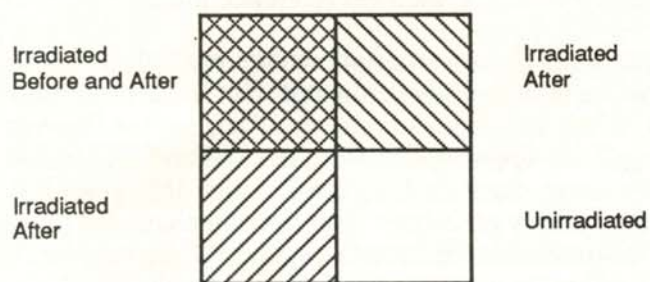


Figure 2.

Regions of the sample resulting from two irradiations with different halves masked at right angles. The irradiation conditions with respect to the film deposition are as marked.

tungsten filament to be accelerated by the Van De Graaf. In the case of the positive ion Van de Graaf, an RF field is applied to a bottle containing a low density hydrogen gas. The resulting collisions generate a hydrogen plasma from which protons can be extracted and accelerated. The particle beam current was maintained at 10-20 mA. For the apertures used, this gives a current density of 2-4 mA/cm². The total dose was measured by integrating the charge deposited on the sample. Doses of 10¹⁷/cm² electrons or protons were typical in this study.

In order to determine whether image charge bonding is an effective mechanism, the order of film deposition and particle irradiation was varied by producing four quadrants of differing irradiation history on each sample. This was done by first masking half of the sample and then irradiating. After the first irradiation, a Cu film was deposited onto the entire sample. Then, the sample was masked again and irradiated, with the mask perpendicular to the initial mask. (See Figure 2.) The result is one quadrant irradiated only before film deposition, one quadrant irradiated both before and after film deposition, one quadrant irradiated only after film deposition, and one quadrant with no irradiation, for reference. If image charge bonding is effective, we expect to see enhanced adhesion in all 3 quadrants which have any irradiation, regardless of the order.

Directly pulling the film from the substrate using a Sebastian[®] pull tester was the method used to test the adhesive strength of the films. The pull test

method is a more quantitative measure film strength than the common adhesive tape test. In the tape test, a piece of adhesive tape is pressed against the film and then pulled off to see whether the film is removed. In the pull test method, a pin of cross sectional area of 7 mm² is cemented onto the film during a low temperature anneal. The stress required to pull the film off is obtained by dividing the force required to pull the pin off by the area of the film removed. The stress is given by the output of the test system, provided that all of the film under the pin head is pulled off. In this study, the film always covered the end of the removed pin; therefore, no adjustment was need for removal of only a portion of the film.

Test cycles consisted of placing a pin on the desired quadrant of each sample, annealing for 90 minutes at 150 C in order to cement the heat sensitive epoxy to the film surface, allowing to cool for 90 minutes, and pulling the pin off with the adhesion tester. Only one pull could be done at a time per physical specimen because the pin is inserted into a hole in a platen with the entire specimen face resting against the platen. The pin is then pulled against the resistance of the platen.

RESULTS

Six samples were made, 3 using electron irradiations, and 3 using proton irradiations. Three test cycles were completed. Pull strengths in the second and third test cycle were significantly weaker than in the first test cycle. Oxidation of the copper film occurred during each annealing cycle. This correlates with the poorer test results obtained from the second and third test cycles.

Of the six samples, four gave measurable results. Three of these gave results only in the first test cycle. The fourth gave results in all three test cycles. It was possible to obtain two pulls representing different irradiation conditions from different pieces of each sample during each test cycle. These sets of results and their irradiation conditions are reported in Table 1. In the table, irradiation conditions are designated by: B - irradiation before film deposition, A - irradiation after film deposition, BA - irradiation before and after film deposition. Of these six sets of pulls, three sets compare irradiation before with irradiation after. All three of these sets showed that irradiation after film deposition results in greater adhesion than irradiation before film dep-

	Cycle 1	Cycle 2	Cycle 3
Proton Irradiation	B 0.03		
	A 6.61		
Proton Irradiation	B 0.0		
	A 0.88		
Electron Irradiation	B 0.54		
	A 5.4		
Electron Irradiation	BA 4.84	BA 0	BA 0
	A 0	A 0.74	A 0.25
Reference Pull 0.13			

Table I

Stress, in 10^3 psi, required to remove the film from the substrate for a given irradiation condition and pull test cycle. Conditions are designated by: B - irradiation before film deposition, A - irradiation after film deposition, BA - irradiation before and after film deposition. The reference pull is from an unirradiated sample.

osition. (First three entries in Table.1) The other three successful sets of pulls compare irradiation after film deposition with irradiation both before and after film deposition. The data obtained in the first test cycle indicates irradiation both before and after film deposition result in greater adhesion than only irradiation after. The results for the second and third test cycles are the opposite. A successful test of an unirradiated sample for reference is also listed in the table.

DISCUSSION

The results indicate that in no case did irradiation before film deposition produce significantly greater adhesion than was measured in the unirradiated case. In four of the six cases of irradiation before film deposition, the adhesion is so weak that no measurable force was required to remove the pin. This would indicate that pre-irradiation may actually degrade the bonding characteristics of the surface. In several cases irradiation after resulted in

greater adhesion than the reference pull.

The pulls from the sample where irradiation both before and after are compared with irradiation only after are ambiguous in that results from the first test cycle are opposite that from the 2nd and 3rd cycles. However, the data from the 2nd and 3rd cycles is more nearly consistent with the other samples in that irradiation before corresponds to degradation in adhesion measurement. Even though it is expected that data from the 1st cycle would be most reliable, given that this is the only case where a sample irradiated before evaporation shows any increased adhesion and that this sample was also irradiated after film deposition, it is reasonable to attribute this increase to irradiation after and the no pull data point to an uncompensated shear.

The absence of increased adhesion due to irradiation before deposition would indicate that image charge bonding is not predominantly responsible for observed adhesion enhancement. This mechanism either does not occur or is too weak to be of any practical importance.

Since ion-beam mixing of the film and substrate was made negligible by the design of the experimental procedure and since image charge bonding does not appear to be effective, the predominant adhesion mechanism involved in this system is concluded to be the formation of interfacial chemical bonds. This is consistent with the fact that the irradiation process provided adequate energy to form ionized atoms near the interface which are needed to form the additional chemical bonds. Also, the degradation of adhesion after heating the samples is consistent with the breaking of metastable bonds during annealing.

ACKNOWLEDGEMENTS

The author would like to thank Dr. Gary Farlow for his valuable guidance and input into this project. Valuable input was also provided by Mr. Wallace Rice, Dr. Jerry Clark, Ernest Williams Jr. and James Robison of Wright State University. He would like to thank the Allied Corporation and the National Society of Physics Students for their support through the 1987 Allied Award, and Ms. Janet Pawel of Oak Ridge National Lab, for her assistance with adhesion measurements.

REFERENCES

1. K. D. Leaver and B. N. Chapman, Thin Films Wykehan Publications, London, 1971.
2. C. W. White, et al., Materials Letters, 2, p. 5A, 1984.
3. J. E. Griffith, et al., Nucl. Instr. Meth., 198, pp. 27-29, (1982).
4. Nicolet, Marc-A., et al., Materials Research Society Symposium Proceedings, Volume 27, Eds. G. K. Hubler, O. W. Holland, C. R. Clayton, C. W. White, Elsevier Science Publishing Co., New York, 1984, p. 3.
5. A. M. Stoneham and P. W. Tasker, Electronic Packaging Materials Science, Eds. E. A. Geiss, K. N. Tu, D. R. Uhlman, North Holland, New York, 1985, p. 11.
6. Paul Lorrain and Dale Corson. Electromagnetic Fields And Waves, W. H. Freeman and Co., New York, 1970, pp, 144 - 156.
7. J. Bottiger, et al., Materials Society Symposium Proceedings, Volume 25, Eds. J. E. E. Baglin, D. R. Campbell, W. K. Chu, Elsevier Science Publishing Co., 1984, p. 203.

FACULTY SPONSOR OF THIS PAPER

Dr. Gary Farlow
Department of Physics
Wright State University
Dayton, OH 45435

THE WEISBUCH/ATLAN MODEL OF IMMUNE RESPONSE

Ulrich Wiesner
Am Brucker Bach 5
D-5060 Bergish Gladbach 1
West Germany

ABSTRACT

Based on the Jerne idea of control of the immune response, a simple immune network of interacting binary automata was presented by Gerard Weisbuch and Henri Atlan¹. The dynamics of this model, put on a 10 x 10 x 10 cubic lattice, is described in this article.

¹ Gerard Weisbuch and Henri Atlan, "Control of the Immune Response", *J. Phys. A, Math. Gen.*, **21**, 1988, pp: L189-192.

INTRODUCTION

If alien substances (antigens such as viruses and macromolecules) invade a body, a strange reaction of the immune system is caused. Millions of different types of pre-existing antibodies (Ab) become responsible for the recognition and destruction of specific antigens.

Antibodies are normally bound to the membranes of white blood cells (B-lymphocytes). If one of these antibodies fits the specific surface of an antigen, the structure of the B-cell changes. The secretion of free antibodies which fit the same antigen is triggered. This proliferation of antibodies leads to the destruction of the antigen.

If isolated antibodies are injected into a foreign body, they cause an immune response and the proliferation of an anti-ideotypic antibody. In the early 1970's, Niels Kai Jerne¹ suspected that this ideotype-anti-ideotype reaction also occurs in an immune system. According to his idea, the immune response is controlled by the following interactions between the parts of the immune system. The increasing number of antibodies (Ab-1) in the presence of an antigen leads to the proliferation of anti-ideotypic antibodies (Ab-2). These antibodies again trigger the secretion of anti-anti-ideotypic antibodies (Ab-3), and so on. To close this circle, it was later shown that Ab-4 (which fits to the Ab-3 surface like the Ab-2) fits in large amounts to the surface of Ab-1. In Jerne's opinion, this internal process is responsible for the control of the immune response. Disorders of this network are the

reason for auto immune diseases.

THE WEISBUCH/ATLAN MODEL

Based on this network approach, Weisbuch and Atlan² introduced a simple immune network consisting of five different cell types (Figure 1) Each automaton, corresponding to low and high concen-

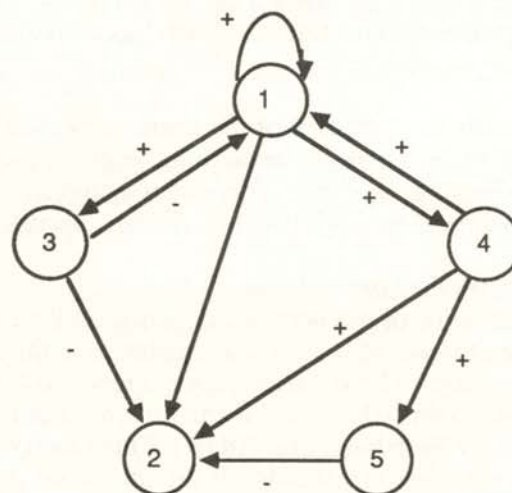


Figure 1

Weisbuch/Atlan model of the immune network. The automata represent resting killer cells (1), activated killer cells (2), T8 suppressor cells (3,5) and T4 helper cells (4).

trations of the equivalent cell type, can assume the binary states 0 or 1. Automaton 1 represents killer cells in a resting state; automaton 2 activated killer cells in the presence of the concerning antigen; automata 3 and 5 represent T8-suppressor cells; automaton 4 refers to T4-helper cells.

Hence, the whole net is able to assume 32 different configurations. The numbers 0 to 31 are assigned to the corresponding binary states. For example, configuration 11 (in binary representation 01011) describes a state with low concentration of both T8-cells and a high concentration of all other cell types.

The configurations are changed in the course of time by parallel updating of the automata. This is done by the addition of the prevailing influence, having a value of 1, -1 or 0 depending upon its suppressing or supporting character. If we demand that for the existence of a 1 in the next step, the sum of the inputs of all cell types has to be larger or equal to 1, the result of the updating is an iteration process with the attracting configurations of 0 and 29. This special threshold is called 'threshold-1'.

Configuration 0 represents the virgin state which does not have any antibodies of the specific antigen. Configuration 29 represents the healthy, vaccinated carrier state, which can be reached only through the critical state 31 which has active killer cells.

Jerne calls the behavior of the immune network caused by its internal interactions 'eigen' behavior of the immune system. The 'eigen' behavior of the Weisbuch/Atlan model will be further discussed.

Behavior of a Simple Network

The behavior of the network depends on the demanded threshold for cellular existence in the following state. The iteration process leads to two attraction basins (0 and 29) if the threshold is 1, as chosen by Weisbuch and Atlan. This changes if we select other thresholds. If the threshold is 2 or greater, the iteration graph leads to attractor 0, independent of the starting state. If the threshold is less than or equal to 0, it leads to attractor 31. State 29, in this case, is not stable and the patient will not survive.

THE 3-DIMENSIONAL CASE

If the Weisbuch/Atlan network is put on a simple

cubic lattice of 10^3 elements, and if each element is influenced by the cells in itself and in its six neighboring elements, we get other results, even though the couplings were the same as in the zero-dimensional case. To reduce the effects caused by the large surface of the cube, cyclic boundary conditions were used. The dynamics of the cube were simulated with a FORTRAN program on a Micro-VAX II.

Each element of the cube is assigned one of the 32 possible states by a random process, each state having the same probability of occurring. Only one threshold allows the existence of two attracting states. If we choose threshold 4, after more than 30 steps, we get about the same number of elements at state 0 as at state 29. Depending upon the initial configuration of the cube, there might be a number of elements switching from one state to the other and then switching back in the next step. A possible structure of an oscillating configuration is shown in Figure 2.

If the threshold is 1, 2 or 3, all elements of the cube reach state 29 after a few steps. If the threshold is less than or equal to 0, the cube reaches state 31 after three steps. If the threshold is 5 or greater, the whole cube takes state 0.

If the probability that a lattice site contains each cell type is reduced from 50% to 20%, we get the same results at thresholds of 0, 1, 2 and 5, but a stable number of about 40 elements at state 0 and a dominant state 0 at threshold 4. These results depend

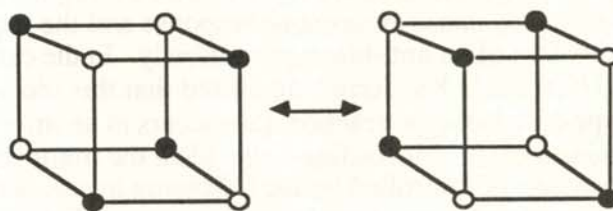


Figure 2

It is possible that the iteration process leads to an oscillating configuration. The filled sites represent state 29, the other sites are at state 0. If the planes above and below the cube are at state 29, the configuration oscillates at threshold 4. If the planes are at state 0, it oscillates at threshold 3.

on the initial configuration of the cube.

Addition of Inert Particles

It is interesting to see how the cube reacts when we introduce inert particles which do not take part in the immune reaction, but fill out some of the cube's elements. If half of the lattice sites are randomly filled with inert cells, and if the remaining sites contain the five other cell types with a probability of 50%, threshold 4 (in contrast to the earlier descriptions) causes the cube to take state 0 after about 4 steps. The thresholds 1 and 3 cause a stable parallel existence of states 0 and 29. At threshold 1, only a very few elements contain a stable state 0. At threshold 3, the number of state 0 elements reaches about 75%. Threshold 0 again causes state 31 after three steps.

If we include inert substances which act as barriers to the cells taking part in the immune reaction, it makes sense to allow the cube elements to be exchanged with their neighbors. This models the mixing of the cells as happens in the blood stream. If we allow at each step for half of the cube element to be exchanged with their neighbors, we get the old results for thresholds 0 and 4. However, we also get the whole cube at state 0 for threshold 3. At threshold 2, we get a varying number of less than 20 elements at state 0 (the other elements become state 29). At threshold 1, no cube elements stay at state 0. The whole cube becomes state 29 after a few steps.

Modeling a Vaccination

This gives rise to an interesting question: which thresholds allow a vaccination of the cube with a small amount of elements in state 1 or 4 that lead to a configuration that contains only elements at state 29? A starting configuration with all elements at state 0 except for a small cube of 3^3 elements at state 1 (representing the injection) should simulate a vaccination.

At threshold 1, the whole cube is at state 29 after 12 steps. However, with thresholds 2,3 or 4, the injected cells change the state of their elements to state 29, but the infection does not spread, so a vaccination is not successful at these thresholds.

These results are different if a number of elements change their positions with neighboring elements after each step. At threshold 2, the whole cube reaches state 29 after about 40 steps if 10% of the elements exchange their position. This process

needs only about 30 steps if 50% of the elements move. With threshold 3, the vaccination is more difficult. If 50% of the elements move after each step, the successful vaccination needs about 90 steps. If only 20 percent change, the infections does not spread. If 75% of the elements change their position, the cube becomes state 0 after a few steps.

An inert portion of only 20% makes a vaccination at threshold 3 impossible. For threshold 2, the 20% inert portion makes the vaccination process slower. If 50% of the cube elements are occupied by non-immune substances, a vaccination needs about 170 steps at 10% movement and about 75 steps at 50% movement. If the non-immune portion increased to 65%, a vaccination is not possible at all.

At threshold 1, a vaccination is prevented only at 75% non-immune parts and only if no motion takes place. If 10% of the cube's elements are exchanged after each step, it needs only 30 steps for a successful vaccination.

In summary, putting the Weisbuch-Atlan model on a simple cubic lattice or a square lattice³ and changing the threshold gives a lot of effects which might be of biological interest.

REFERENCES

- 1 Niels Kai Jerne, "The Immune System", *Sci. Am.* 229, July 1973.
- 2 Gerard Weisbuch and Henri Atlan, "Control of the Immune Response", *J. Phys. A.: Math. Gen.*, 21, 1988, pp. L189-192.
- 3 Ito Dayan, Dietrich Stauffer, Shlomo Havlin, "Cellular Automata Generalization of Weisbuch-Atlan Model for Immune Response", *J. Phys. A, Math. Gen.*, 21, pp 2473-2476.

FACULTY SPONSOR

Professor Dietrich Stauffer
Institute of Theoretical Physics
University of Cologne
D-5000 Koln
West Germany

MONTE CARLO SIMULATION OF A HIGH PRESSURE PROPORTIONAL COUNTER

Zoltan Egyed
Department of Physics
Eotvos University, Budapest, Hungary
and
Union College, Schenectady, New York

ABSTRACT

The Monte Carlo method is a computational technique for simulating a complex system's behavior. The method was used to predict the output of a high pressure proportional chamber with a Cd^{109} source and different gas pressures. A brief introduction to the chamber and the method is included.

INTRODUCTION

This work is part of a research project on high pressure gas detectors which is performed at Union College in collaboration with Lawrence Berkeley Laboratory and New York University¹. The final goal the project is a high pressure time projection chamber (TPC) which gives great efficiency and the ability to reconstruct the track in 3 dimensions by the time projection method.

A TPC has a good energy resolution and a big energy loss for charged particles, making it good for particle identification². The big energy loss is due to the high pressure which gives more matter to interact with the particle.

As a first step, we are investigating the behavior of high pressure proportional chambers. A particularly interesting characteristic is the detection efficiency for X-rays. There are two possible approaches to study the problem: experiments and computer simulation. Agreement between the results of these methods would show that we understand the physical processes in the detector. This article describes a program which uses the Monte Carlo method to simulate the behavior of the detector.

THE MONTE CARLO METHOD

Let us assume that one wants to calculate an integral of a function. There are different ways to do that. One can look up the integral in an integral table, but many functions one uses in real life do not appear in these tables. Sometimes one has to use some sort of approximation to calculate the integral. There are several methods for doing this. One can take the values of the function at different points and use the rectangle method or Simpson's formula. One can also use a totally different method, namely computer simulation³.

This method is based on a "random number generator". Using it, the computer chooses lots of numbers between the two boundary values. Every equal interval between the two boundary values has the same probability to get chosen. To use this method to calculate an integral of a function of one variable, you make its graph (see Figure 1), and pick a point randomly on the picture. You determine if the point is above or below the function. This is repeated a large number of times, picking a random point and determining if it is above or below the function. As the number of trials increases, the distribution of points will become more homogeneous. The ratio of the area under the curve

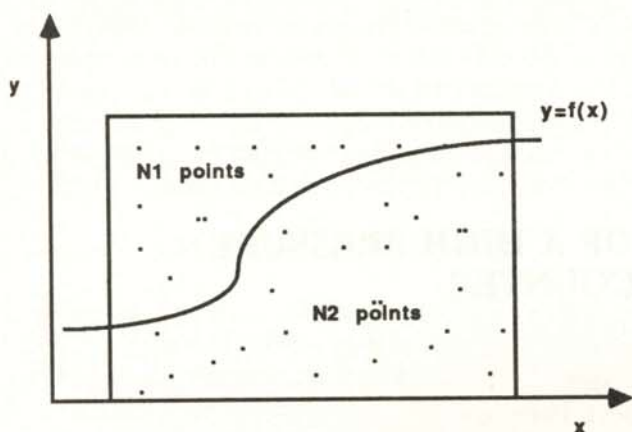


Figure 1
Monte Carlo method in two dimensions.

to the total area is approximately equal to the ratio of the number of points under the function to the total number of points. If you know the total area, then you know the area under the graph and the integral of the function. This value is not exact. To get a more accurate solution, the program needs more tries. If you have N points under the graph, the relative error will be about $N^{-1/2}$.

The same method works in three dimensions. To calculate the volume inside some closed three dimensional surface (see Figure 2), a bigger volume enclosing it is chosen, for instance a cube. The same procedure as for the two dimensional case is repeated. Points inside this cube are chosen randomly and hence will be distributed approximately homogeneously inside the cube. The ratio of the volumes inside and outside the closed surface is approximately the same as the number of points inside and outside the surface.

This seems to be an inefficient way to solve the problem, but if one has a function of more variables, this method becomes the most practical one because of the calculating speed of modern computers. One has often to work with several hundred or thousands of variables. If one does not have a "nice" function, it cannot be analytically integrated easily. In such a case, the Monte Carlo computer simulation method will work well.

This method can be used in different problems. To calculate the effectivity of a system, which can be almost anything from particle detectors to nuclear submarines, the influences which act on the system are simulated and the results found. To have a

good idea about the system's behavior, a large number of possibilities have to be included.

Simulating the Detector

To simulate the behavior of a detector, a large number of particles with different properties such as direction and energy are generated. As the operation of the detector is simulated, the behavior of the system becomes obvious.

Our detector is a high pressure proportional chamber (shown in Figure 3). On the top of it is a radioactive Cd^{109} source. The cadmium decays by electron capture to Ag^{109} . When the electron is captured, a proton in the nucleus of the Cd atom is changed to a neutron and a neutrino is emitted. The Ag nucleus is left in an excited state. This nucleus then decays to its ground state by emitting a X-ray photon. This emission is dominated by three energies (22 keV, 25 keV and 88 keV) with different probabilities.

These photons can go in any direction. They have different absorption lengths in the wall of the detector and in the gas inside. If the photon travels through the wall and is absorbed in the gas, it will give a free electron and a positively charged ion. The high voltage between the wire and wall will cause an electric field which will accelerate the electron towards the wire. If the electron is traveling fast enough, it can ionize another gas atom. The new electron is accelerated as well and the process repeats itself, creating an avalanche of electrons hitting the wire. This gives a measurable electric pulse.

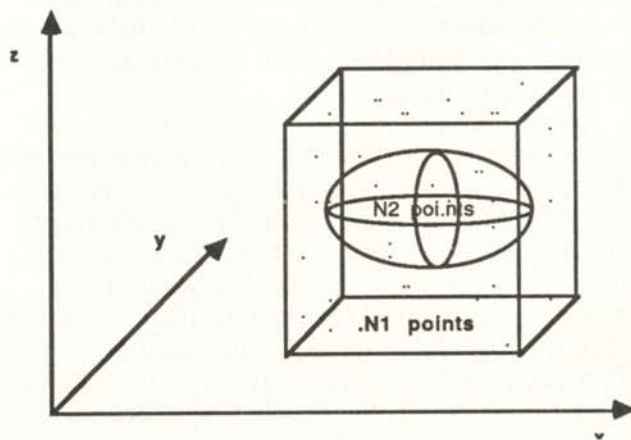


Figure 2
Monte Carlo method in 3 dimensions.

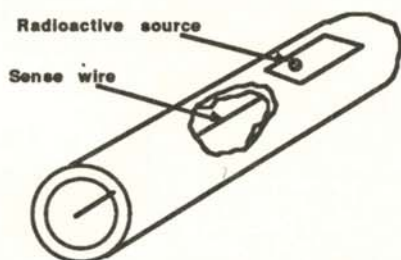


Figure 3
The high pressure proportional chamber.

If the photon is absorbed in the wall, there will not be any output from the detector. If a photon does through the wall and through the gas, it won't give any signal.

The Program

A key question to answer is how many photons will be absorbed in the gas inside the detector at the various energies. The photons of different energies have different absorption lengths in the wall and in the gas. To simulate the motion requires 4 randomly chosen parameters: the energy of the photon; two direction angles and the point of absorption.

The Monte Carlo program generates the photon energies with the given probabilities, gives a direction to the photon, decides if the photon is absorbed in the wall (by the distance it has to travel inside it) and decides if it is absorbed in the gas. This process is done typically a million times. The program gives the ratio between the number of 88 keV photons detected and the sum of the number of 22 and 25 keV photons detected. The calculation is done for different gas mixtures and gas pressures inside the detector. This predicts the spectrum without having to do a long costly experiment at every parameter value.

The method helps to calculate other parameters of the system too. On top of the detector, between the Cd^{109} source and the gas, there is a thin brass window. The thickness of it is very hard to measure because it is deep inside the detector. Its nominal value was 0.008 inches. It turned out that the simulation is a very sensitive tool to measure this thickness. Given the different values for energy and pressure, the Monte Carlo program determined the window thickness to be 0.005 inches.

We compared the program results with data from

the detector at a few parameter settings. The results of the simulation, shown in Figure 4, agree well with measured values. This indicates that we understand the physical processes in the detector. We can use the program to predict the spectrum at different gas compositions and different pressures.

ACKNOWLEDGMENTS

The author wishes to thank Dr. Laszlo Baksay for providing support for this work. The author would also like to thank the Computer Center of Union College for giving a large amount of CPU time on their VAX computers.

REFERENCES

1. P. Oddone, G. Smith, A. Green, P. Nemethy, L. Baksay, L. Schick, E.G. Heflin, "Development of High Pressure Proportional Counters", Nuclear Instruments and Methods in Physics Research A252, 1986.
2. E. Heflin, "Development work towards a high pressure time projection chamber", Bachelor Thesis, University of Dallas, 1985.
3. I. Manno, "A Monte Carlo módszer kiserleti reszecskefizikai alkalmazasanak alapja" Hungarian Academy of Sciences, 1986.

FACULTY SPONSOR

Dr. Laszlo Baksay
Department of Physics
Union College
Schenectady, NY 12308

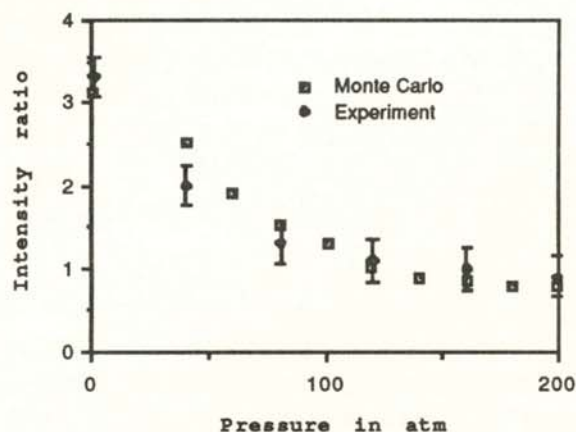


Figure 4
Experimental and computational results.

SUPERIONIC-COVALENT PHASE TRANSITIONS IN ALLOYS OF Ag_3SI with Ag_3SBr

Eric Moen, Greg Schurter and Ivan Wick
Department of Physics and Astronomy
University of Wisconsin-Stevens Point
Stevens Point, WI 54481

ABSTRACT

Polycrystalline alloys of Ag_3SI with Ag_3SBr were prepared from the melt and analyzed with X-ray diffraction and electric conductivity techniques. The measured lattice parameters simply follow Vegard's Law as a function of composition. The transition temperature separating the superionic and insulating phases of these alloys remains constant in the iodide-rich region and varies linearly with composition in the bromide-rich region.

INTRODUCTION

Fast ion conductors continue to be of interest to solid state physicists since the first one (PbF_2) was discovered by Michael Faraday in 1834¹. In these compounds, which are also referred to as superionic conductors or solid electrolytes, one of the ionic species is able to move relatively freely at elevated temperatures throughout the crystal lattice resulting in high electric conductivity. Typically, a transition temperature separates the superionic state from a low temperature insulating (covalent) state in which all ions within the crystal are essentially confined to lattice sites.

Silver based solid electrolytes have been of particular interest. Shahi and Wagner² found that chemical substitution in the fast ion conductor AgI produced effects similar to pressurization. As the bromide anion was substituted for iodide in this compound or when hydrostatic pressure was exerted on this compound, the superionic-covalent transition temperature was depressed in a linear fashion. This seemed reasonable if the smaller bromide anion compresses the lattice just as pressurization would. However, Shahi and Wagner, based on a theoretical model developed by Rice, Strassler and

Toombs³, suggest that the substitution of even a larger anion may produce the same depression of the transition temperature as bromide substitution. Unfortunately, no larger single-valence anion exists for such a test with AgI . However, other solid electrolytes may be studied to investigate this prediction. The alloy system $\text{Ag}_3\text{SI}_{1-x}\text{Br}_x$ permits bromide substitution for iodide in Ag_3SI as well as iodide substitution for bromide in Ag_3SBr .

Ag_3SI and Ag_3SBr are both fast ion conductors at room temperature with identical cubic crystal structures. Ag_3SI changes to a covalent, rhombohedral crystal at 157K, while Ag_3SBr changes to a covalent, tetragonal crystal at 126K⁴. Electric conductivity measurement show associated discontinuous changes at these transition temperatures⁵.

Very little work has been done to characterize the properties of alloys in the series $\text{Ag}_3\text{SI}_{1-x}\text{Br}_x$. Reuter and Hardel⁶ found that uniform alloys are formed throughout the composition parameter range $x = 0$ to $x = 1$. Sakuma, Fujishita, and Hoshino⁷ found a crystallographic phase transition in $\text{Ag}_3\text{SI}_{0.5}\text{Br}_{0.5}$ at a temperature of 115K although

the cryogenic structure seems to be different from the low temperature phases of either Ag_3SI or Ag_3SBr .

EXPERIMENTAL DETAILS

High purity AgI , AgBr and Ag_2S were used as received from Johnson Matthey Aesar. Stoichiometric quantities of each were sealed in evacuated quartz tubes, melted together at 800°C and then cooled naturally to room temperatures. X-ray diffraction patterns taken at this point produced rather faint, diffuse lines, indicating a somewhat glassy material. The samples were subsequently powdered, pressed into pellets and resealed in evacuated quartz tubes. These tubes were reheated at 200°C for one month. After this annealing period, the diffraction lines were sharp and clear.

The X-ray data were taken with a 114.6 mm Debye-Scherrer camera using Cu radiation of wavelength 1.54178 \AA . The lattice parameters that are reported for each sample were obtained by averaging those values calculated from the six most intense diffraction lines in each photograph. The standard deviations of the averaged lattice parameters never exceeded 0.008 \AA .

The transition temperatures were found using a locally constructed cryostat. The cryostat could be operated from 120 - 300 K using an Omega Engineering controller. The temperature was both controlled and measured to a stability of 0.5K with a

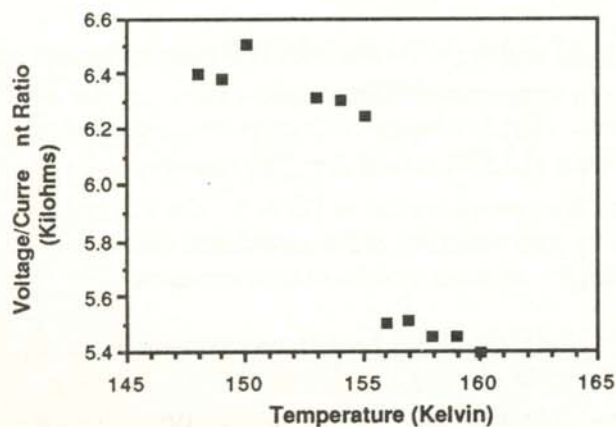


Figure 1

The ratio of measured voltage to current as a function of temperature for a typical $\text{Ag}_3\text{SI}_{1-x}\text{Br}_x$ alloy sample.

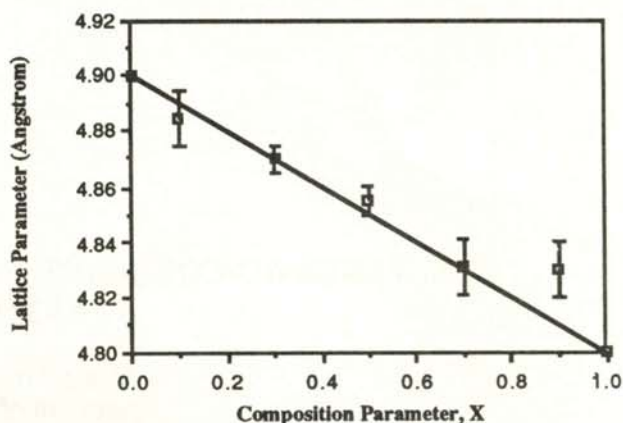


Figure 2

Lattice parameter versus composition in the $\text{Ag}_3\text{SI}_{1-x}\text{Br}_x$ alloy series. The line is the prediction of Vegard's Law.

Chromel-Alumel thermocouple with placed along side the sample. The alternating current from a 1000 Hertz sine wave generator passing through the sample as well as the voltage developed across the sample were measured with a Keithly Model 177 digital multimeter. The ratio of voltage to current provided a rough measure of the sample resistance. This was sufficient to determine the transition temperatures. Figure 1 is a representative voltage-current ratio vs temperature curve for one of the sample pellets. The measurement of the actual sample resistance would require a vector impedance meter⁸ which was not available for this study.

RESULTS

The lattice parameters of our prepared alloys in the $\text{Ag}_3\text{SI}_{1-x}\text{Br}_x$ series are presented in Figure 2. The error bars indicate standard deviations of the calculated means. The values plotted for pure Ag_3SI and Ag_3SBr were taken from the work of Reuter and Hardel⁶. The line connecting these two lattice parameters represents Vegard's Law. Vegard's Law predicts the value of the lattice parameter from a simple hard-sphere mixing of appropriate proportions of iodide and bromide with sulfide and silver ions. Within the experimental uncertainty, our data follows Vegard's Law.

Figure 3 illustrates the variation in superionic-covalent transition temperature with alloy composition. The error bars include both temperature sta-

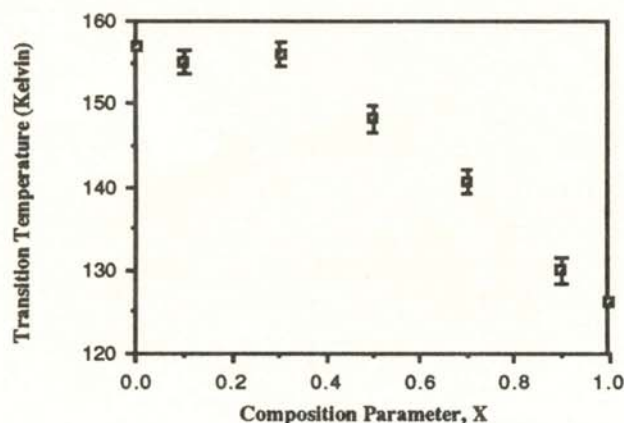


Figure 3

Superionic-covalent phase transition temperature versus composition in the $\text{Ag}_3\text{SI}_{1-x}\text{Br}_x$ alloy series.

bility of the controller and the width of the transition. The transition temperatures of pure Ag_3SI and Ag_3SBr were obtained from Hoshino et. al. 9. The measured temperatures of our alloys suggest a nearly constant value for x less than 0.3 and a linear decrease for x greater than 0.3. The 148K transition temperature obtained for the $x = 0.5$ sample differs significantly from the 115K value found previously⁷ although it does fit the pattern established by its neighboring alloy samples in this study. Unfortunately, the minimum attainable temperature of our cryostat was approximately 120K, so we were not able to check for any additional anomalies near 115 K.

CONCLUSION

Shahi and Wagner² suggested that substitution of a larger anion into the lattice of a superionic conductor may result in a depressed transition temperature based on their work with chemically substituted AgI . Our results do not confirm this for the case of iodide substituted Ag_3SBr . As the larger iodide anion is substituted for bromide in Ag_3SBr (i.e., as composition parameter x decreases from 1.0), we observe an increase in the transition temperature. Even in the case of bromide substituted Ag_3SI (as x increases from 0.0), we find that chemical substitution produces results markedly different from bromide substituted AgI .

It would be of interest to compare the effect of chemical substitution on the magnitude of electric conductivity of Ag_3SI and Ag_3SBr with the more widely studied case of AgI . Toward this end, we are currently improving our electrical measurement capability to permit precise impedance determinations for such an investigation.

ACKNOWLEDGMENT

This research was supported by a grant from the Research Corporation.

REFERENCES

1. D.F. Shriver and G.C. Farrington, Chem. Eng. News, 43, May 20, 1985.
2. K. Shahi and J.B. Wagner, Phys. Rev. B, 23, 1981, p. 6417.
3. M.J. Rice, S. Strassler and G.A. Toombs, Phys. Rev. Lett., 32, 1974, p. 596.
4. G. Spinolo and V. Massarotti, Z. Phys. Chem. Neue Folge, 121, 1980, p. 7.
5. G. Chiodelli, A. Magistris and A. Schiraldi, Z. Phys. Chem. Neue Folge, 118, 1979, p. 177.
6. V.B. Reuter and K. Hardel, Z. Anorg. Allg. Chem., 340, 1965, p. 158.
7. T. Sakuma, H. Fujishita, and S. Hoshino, Phys. Soc. Jpn., 51, 1982, p.s 2628.
8. R.J. Cava and E.A. Rietman, Phys. Rev. B, 30, 1984, p. 6896.
9. S. Hoshino, H. Fujishita, M. Takashige and T. Sakuma, Solid State Ionics 3/4, 1981, p. 35.

FACULTY SPONSOR

Professor Robert Beeken
Department of Physics and Astronomy
University of Wisconsin-Stevens Point
Stevens Point, WI 54481

POST USE BOOK REVIEW

CLASSICAL MECHANICS by A. Douglas Davis
Academic Press, Inc., 1986

CLASSICAL DYNAMICS OF PARTICLES AND SYSTEMS, 2nd Ed. by Jerry B. Marion
Harcourt Brace Jovanovich, 1970

Reviewed by:

G. Douglas Meegan, Jr.
Guilford College, Greensboro, NC 27410

Classical Mechanics, by A. Douglas Davis, is primarily intended to be a sophomore level text which prides itself on clarity and detail. However, this text is somewhat limited in that its presentation of the material is strictly designed to be introductory. In comparison, *Classical Dynamics of Particles and Systems*, by Jerry B. Marion, lends itself to the developing physicist as a text for future reference as well as a teaching tool.

Many factors must come into play when a physics text is chosen. For example, students are most often concerned with the readability of a text. Some students and professors of physics prefer a text that places the stress upon achieving good intuition of physical phenomena, while others prefer a text which presents the mathematical foundations of physical phenomena in great detail and with little 'hand waving'.

Classical Dynamics of Particles and Systems, by Marion, does indeed present the thorough mathematical foundations of mechanics and, therefore, must be recognized as a more advanced text designed for use by students which require little if any further study of the fundamental techniques of calculus. However, Marion's text does not readily lend itself as a teaching device for self-study and

must often be further expounded by an instructor. For these reasons, Marion's text is better suited for the more advanced undergraduates at, perhaps, the junior level.

Unfortunately, Marion's text does suffer a few drawbacks. The text has rather complicated exercises which are left for the student. Quite often, even the first problem at the end of a chapter is difficult and requires further explication by an instructor. As a contributing factor, Marion's text lacks sufficient examples, especially in the latter chapters which are seemingly devoid of them all together. The text does, however, serve its purpose as a reference book through its distinct sectioning, proper use of appendices, and a sufficient index.

In contrast to Marion's text, *Classical Mechanics*, by Davis, presents itself to the reader with an emphasis on developing the students' physical intuition throughout the text with the use of plentiful illustrations and graphs. This text, unlike Marion's, does not assume a mastery of the fundamental techniques of calculus. Davis' book applies these ideas to the physical situations found throughout classical mechanics. He reinforces the usefulness of mathematics and its relationship with physics. By doing so, Davis prevents the possible confusion that the reader might experience when introducing new mathematical techniques like those found throughout Marion's text. The Davis text is much more suited for the less advanced undergraduate.

Doug is a senior physics major from Delmar, New York. His hobbies include percussion and keyboard studies and he has regularly performed with the Greensboro College Stage Band. He hopes to study acoustical physics in graduate school.

In being primarily designed as a teaching device rather than a reference book, Davis' text is complemented by a wider range of exercises which are left for the student. The text is less mathematical than

Marion's. The derivations and formulations presented in the Davis text are usually adequate for the completion of the problems found at the end of each chapter. The material within the text is presented in an order appropriate for presentation to a class. For example, Davis presents most of the mathematical tools used in classical mechanics throughout the text, rather than lumping them together in a single chapter and a few appendices as Marion has done to some extent. Davis' text may be best suited in a class whose instructor lacks sufficient ability, technique or desire to explain the material.

Despite its readability and other appealing characteristics, *Classical Mechanics*, by Davis, suffers some significant drawbacks. My primary dissatisfaction with the text is its introductory foundations. As Davis has suggested in his "Preface," the text is designed to be used by students of several disciplines including engineering and the sciences in general. Rather than having use as a reference tool, *Classical Mechanics*, by Davis, solely provides the student with an introductory understanding of the material. (I have found little use for this text since I completed the introductory course in mechanics close to two years ago!)

On the contrary, Marion has created a text which is mathematically more formal than Davis' text while simultaneously being much more inclusive of several advanced ideas (mathematical and physical) found throughout classical mechanics. *Classical Dynamics of Particles and Systems*, by J. B. Marion, is a superior text which successfully serves its purpose as an introductory text as well as a more advanced text capable of thoroughly preparing a student for graduate studies in physics.